Bundle Sheath Diffusive Resistance to CO_2 and Effectiveness of C_4 Photosynthesis and Refixation of Photorespired CO_2 in a C_4 Cycle Mutant and Wild-Type *Amaranthus edulis*[1]

Olavi Kiirats, Peter J. Lea, Vincent R. Franceschi, and Gerald E. Edwards*

School of Biological Sciences, Washington State University, Pullman, Washington 99164–4236 (O.K., V.R.F., G.E.E.); and Department of Biological Sciences, Lancaster University, Lancaster LA1 4YQ, United Kingdom (P.J.L.)

A mutant of the NAD-malic enzyme-type C_4 plant, *Amaranthus edulis*, which lacks phospho*enol*pyruvate carboxylase (PEPC) in the mesophyll cells was studied. Analysis of CO_2 response curves of photosynthesis of the mutant, which has normal Kranz anatomy but lacks a functional C_4 cycle, provided a direct means of determining the liquid phase-diffusive resistance of atmospheric CO_2 to sites of ribulose 1,5-bisphosphate carboxylation inside bundle sheath (BS) chloroplasts (r_{bs}) within intact plants. Comparisons were made with excised shoots of wild-type plants fed 3,3-dichloro-2-(dihydroxyphosphinoylmethyl)-propenoate, an inhibitor of PEPC. Values of r_{bs} in *A. edulis* were 70 to 180 $m^2\ s^{-1}\ mol^{-1}$, increasing as the leaf matured. This is about 70-fold higher than the liquid phase resistance for diffusion of CO_2 to Rubisco in mesophyll cells of C_3 plants. The values of r_{bs} in *A. edulis* are sufficient for C_4 photosynthesis to elevate CO_2 in BS cells and to minimize photorespiration. The calculated CO_2 concentration in BS cells, which is dependent on input of r_{bs}, was about 2,000 μbar under maximum rates of CO_2 fixation, which is about six times the ambient level of CO_2. High re-assimilation of photorespired CO_2 was demonstrated in both mutant and wild-type plants at limiting CO_2 concentrations, which can be explained by high r_{bs}. Increasing O_2 from near zero up to ambient levels under low CO_2, resulted in an increase in the gross rate of O_2 evolution measured by chlorophyll fluorescence analysis in the PEPC mutant; this increase was simulated from a Rubisco kinetic model, which indicates effective refixation of photorespired CO_2 in BS cells.

In C_4 plants, atmospheric CO_2 is fixed via phospho*enol*pyruvate carboxylase (PEPC) in mesophyll cells into C_4 acids, which are transported to bundle sheath (BS) cells where they serve as donors of CO_2 to the C_3 cycle via C_4 acid decarboxylases (Kanai and Edwards, 1999). Photosynthetic carbon metabolism in C_4 plants requires low rates of CO_2 leakage from BS cells for CO_2 to be concentrated around Rubisco in the BS chloroplasts. This favors CO_2 fixation and minimizes photorespiration. However, the BS is not impermeable to gases because there is a need for metabolites to be exchanged between it and the mesophyll cells and for O_2 generated during photosynthesis to be released. This permeability causes CO_2 leakage from BS cells and results in a lower energetic efficiency of the CO_2-concentrating mechanism.

Diffusive resistance of CO_2 into BS cells (r_{bs}) has been estimated by measuring photosynthetic rates under varying CO_2 concentrations in isolated BS cells (Furbank et al., 1989) and in excised leaves fed a chemical inhibitor of the C_4 cycle (Jenkins et al., 1989a; Brown and Byrd, 1993; Brown, 1997), or by applying models to experimental data related to the magnitude of photorespiration in C_4 plants (He and Edwards, 1996). However, accurate determination of r_{bs} is difficult; current estimates vary over a wide range from about 15 to 1,400 $m^2\ s^{-1}\ mol^{-1}$ (for review, see He and Edwards, 1996).

BS-diffusive resistance is considered the major component that determines the CO_2 leakage driven by the CO_2 concentration gradient between BS and mesophyll cells. The rate of leakage of CO_2 from the BS cells is equal to the rate of over-cycling of the C_4 pathway (rate of C_4 cycle minus rate of CO_2 fixation by the C_3 cycle). There is considerable variation in estimates of the fraction of CO_2 leakage with various methods, ranging from 0.08 up to 0.5 when expressed as a fraction of C_4 cycle activity (see He and Edwards, 1996). CO_2 leakiness was determined for a number of species using an isotope discrimination method (Henderson et al., 1992) and a method involving analysis of $^{14}CO_2$ release after its fixation (Hatch et al., 1995), with leakiness values ranging from 0.08 to 0.3.

The CO_2 concentration in BS cells is dependent on r_{bs}, the rate of C_4 pathway over-cycling, and the CO_2 diffusion gradient from BS to mesophyll cells. For a better understanding of C_4 photosynthesis, it would also be valuable to know the actual CO_2 concentration in BS chloroplasts, where CO_2 assimilation takes

[1] This research was supported by the National Science Foundation (grant nos. IBN–9807916 and IBN–0131098 to G.E.E.).

* Corresponding author; e-mail edwardsg@wsu.edu; fax 509–335–3184.

Article, publication date, and citation information can be found at www.plantphysiol.org/cgi/doi/10.1104/pp.008201.

place. A possible means of estimating this is to combine measurements of CO_2 fixation with information on the kinetic properties of Rubisco. Ribulose 1,5-bisphosphate (RuBP) carboxylation and oxygenation in BS chloroplasts are competing reactions, and information is available on the Rubisco CO_2 to O_2 affinity ratio.

In this study, we have used the PEPC mutant of *Amaranthus edulis* LaC_4 2.16 (Dever et al., 1995; Maroco et al., 1998a, 1998b), which has a defective C_4 cycle and requires direct diffusion of atmospheric CO_2 into the BS cells for CO_2 assimilation and growth. In this mutant, the primary carboxylase for fixing atmospheric CO_2 is Rubisco, which is located in the BS chloroplast. The purpose of this work was to use gas exchange measurements on the *A. edulis* mutant for direct estimation of BS cell resistance to CO_2, and to determine the dependence of r_{bs} on the developmental stage of the leaf. For comparison, data were also obtained with wild-type plants by feeding the PEPC inhibitor 3,3-dichloro-2-(dihydroxyphosphinoyl-methyl)-propenoate (DCDP) to prevent operation of the C_4 cycle. In addition, we determined rates of CO_2 fixation and gross rates of O_2 evolution to analyze the effect of temperature on the cellular conductance to CO_2 and the effects of CO_2, light, and O_2 on partitioning of electron flow and refixation of photorespired CO_2.

RESULTS AND DISCUSSION

Figure 1 outlines important aspects of photosynthesis in the PEPC mutant of *A. edulis* relative to the experimental approach for determining the BS-diffusive resistance to CO_2 (r_{bs}). Because the C_4 cycle is inoperative, the mechanism of CO_2 fixation and energy requirements are considered the same as in C_3 plants. Fixation of atmospheric CO_2 in the mutant by Rubisco in the C_3 cycle, requires diffusion of CO_2 from the mesophyll to BS cells. CO_2 is considered the primary species of inorganic carbon diffusing to BS cells and supplying CO_2 to Rubisco. Although CO_2 will be converted rapidly to bicarbonate in the cytosol of mesophyll cells via carbonic anhydrase, the diffusion pathway for bicarbonate will be limited because it is not used by Rubisco and BS cells lack, or have negligible levels of, carbonic anhydrase (Ku and Edwards, 1975). Also, in wild-type *A. edulis*, where CO_2 is concentrated in the BS cells by the C_4 cycle through C_4 acid decarboxylation, CO_2 is considered the primary form of inorganic carbon leaking from BS to mesophyll cells (Jenkins et al., 1989b). Reaction of O_2 with RuBP in the photosynthetic carbon oxidation cycle in the BS chloroplasts will result in the production of the photorespiratory products glycerate, CO_2, and ammonia through metabolism in mitochondria and peroxisomes. According to the known compartmentalization of carbon assimilation in C_4 plants (Kanai and Edwards, 1999), the only function of mesophyll chloroplasts in carbon assimilation in the mutant may be the conversion of glycerate, the product of photorespiration in BS cells, to triose phosphate and conversion of some of the 3-phosphoglycerate (PGA), generated by Rubisco in BS cells, to triose phosphate.

BS-Diffusive Resistance to CO_2 (r_{bs})

The resistances involved in uptake of atmospheric CO_2 by the mutant are described in Equation 10 ("Materials and Methods"). If the CO_2 response curve of CO_2 assimilation (measured at light saturation) is plotted against the intercellular CO_2 partial pressure (C_i), which equilibrates with the liquid phase at the cell wall, the initial slope of the curve is determined by the average physical liquid phase conductance and by the carboxylation efficiency of Rubisco (Fig. 2). Gas phase resistance to CO_2, r_s, was calculated based on transpiration measurements. Typical values of r_s for the mutant plants were in the

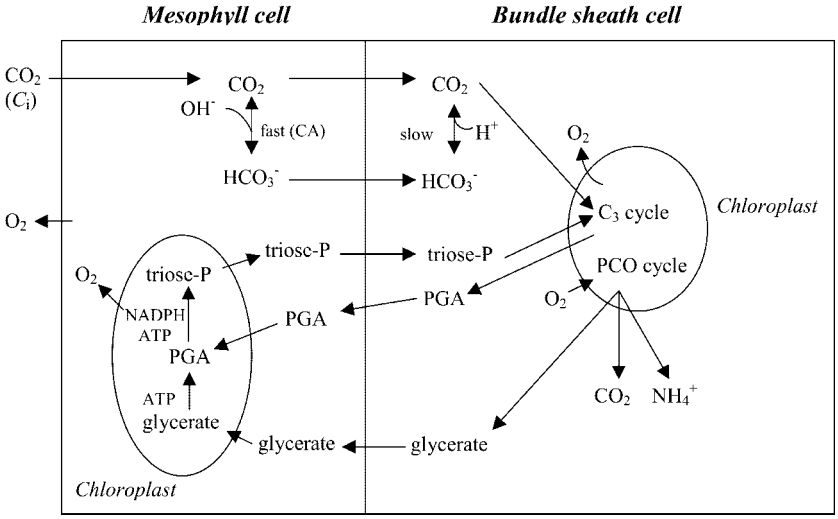

Figure 1. Schematic representation of the movement of gases and metabolites in the PEPC mutant of *A. edulis*. CO_2 diffuses into BS cell chloroplasts where it enters the C_3 cycle. Equilibrium between HCO_3^- and CO_2 in mesophyll cell is fast, but it is slow in BS because of lack of carbonic anhydrase activity. Glycerate, ammonia, and CO_2 are generated by the photosynthetic carbon oxidation (PCO) cycle. Glycerate metabolism and partial reduction of PGA in mesophyll cells may account for use of some photochemically generated energy in mesophyll chloroplasts.

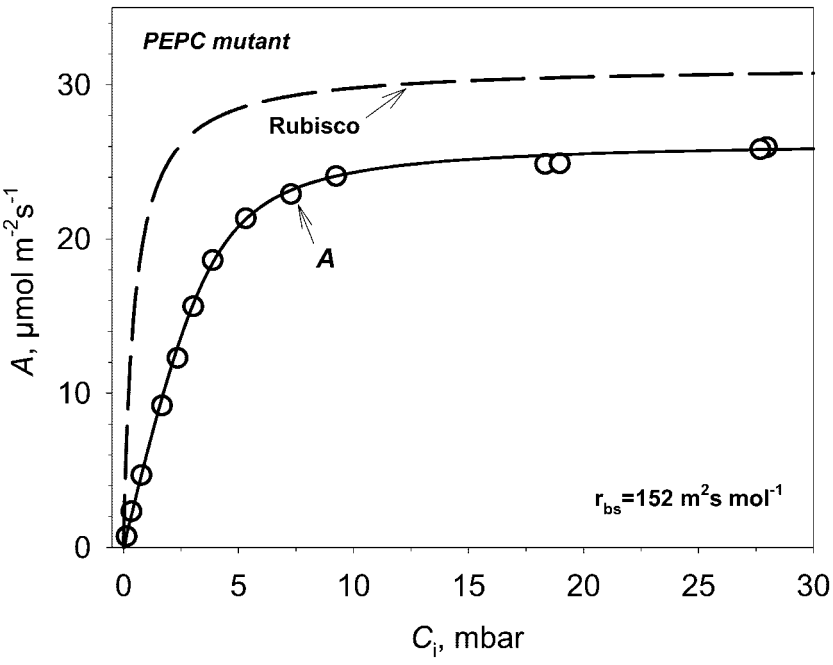

Figure 2. Example of calculating BS cell resistance from A versus C_i curves measured at low O_2 (0.3 mbar) and PFD of 1,800 μmol m^{-2} s^{-1} in PEPC mutant. The inverse of the initial slope of A/C_i curve is the sum of the diffusive resistance from the cell wall to the sites of Rubisco and of the chemical RuBP carboxylation resistance. A simulated Rubisco CO_2 response curve without diffusive resistance is shown for comparison. Rubisco resistance can be calculated as K_c/V_c. V_c was taken as A_{max}.

range of 5 to 10 m^2 s^{-1} mol^{-1} (2–4 s cm^{-1}). Also, the expected Rubisco CO_2 response curve is shown in Figure 2 in the absence of liquid phase resistance; this demonstrates the contribution of the resistance of RuBP carboxylase (chemical resistance), r_c, to the total CO_2 flux resistance. The Rubisco response was generated taking the maximum velocity of RuBP carboxylase (V_c) as 1.2 times the CO_2-saturated rate of CO_2 fixation (A_{max}) based on Rubisco extractable activity measurements. Also, there is a decrease in RuBP pool with increasing CO_2, which could account for A_{max} being lower than V_c of Rubisco if RuBP becomes limiting (as shown later in Fig. 7). In general, r_c for mutant leaves was a minor component (from 10 to 15 m^2 s^{-1} mol^{-1}) compared with r_{bs} (152 m^2 s^{-1} mol^{-1} in Fig. 2).

Analogous experiments to those in Figure 2 were performed on leaves of different maturity. The value of r_{bs} increased with plant age and reached its highest value during grain filling when the leaves were pale green, showing early signs of senescence and lower maximum rates of CO_2 fixation (Table I). Although BS resistance was calculated assuming V_c is 1.2 times A_{max}, a sensitivity analysis taking V_c/A_{max} = 1.0 and 1.4 showed that this results in a change in the calculated r_{bs} values of only 3% to 5% in young leaves, and approximately 2% in mature leaves. Interestingly, during the grain filling stage, the leaves still maintained a reasonably high-CO_2 assimilation capacity. The liquid phase resistance from the mesophyll cells to Rubisco in the mutant *A. edulis* (72–181 m^2 s^{-1} mol^{-1}; Table I) is about 70-fold higher than that of C_3 plants (approximately 1–3 m^2 s^{-1} mol^{-1}; Evans et al., 1994; Laisk and Loreto, 1996). This high-diffusive resistance in C_4 plants may be attributed to the relatively low BS cell surface area per unit leaf area and structural properties of BS cell walls (Evans and von Caemmerer, 1996). Models of C_4 photosynthesis indicate the rate of CO_2 assimilation under low CO_2 drops rapidly below r_{bs} values of 50 to 100 m^2 s^{-1} mol^{-1}

Table I. *Leaf age-dependent differences in A_{max} and resistance to CO_2 in the A. edulis PEPC mutant plants*

The mesophyll to BS resistance for CO_2 was calculated as the inverse of the initial slope of A/C_i curves. The SD for mesophyll to BS resistance and A_{max} was calculated from four independent measurements. r_{bs} was calculated according to the method used in Figure 2. A_{max} was the CO_2-saturated rate of photosynthesis, and other conditions of the assay were as in Figure 2.

Leaf Description	A_{max}	Mesophyll to BS Resistance to CO_2 (r_{bs} + r_c)	Liquid Phase Resistance to CO_2 (r_{bs})
	μmol m^{-2} s^{-1}	m^2 s^{-1} mol^{-1}	
Young, 30% expanded	25.1 ± 1.4	89 ± 16	72.4
Young, 70% expanded	26.6 ± 1.8	103 ± 16	86.3
Mature, vegetative, 100% expanded	30.6 ± 1.0	127 ± 6	113.4
Grain filling stage, 100% expanded	20.6 ± 1.2	201 ± 17	180.8

(Edwards et al., 2000; Laisk and Edwards, 2000; von Caemmerer, 2000).

The resistance observed in the mutant might not reflect the true value of the wild type if the mutation alters the structure of the BS cells. To test this, we used the PEPC inhibitor DCDP, feeding it into the petiole to block the C_4 cycle in wild-type plants (method of Jenkins et al., 1989a). The strong reduction in carboxylation efficiency caused by 4 mM DCDP, without a biphasic response (Fig. 3), suggests that PEPC is almost completely inhibited. CO_2 response curves were measured at 2% (v/v) O_2 before applying DCDP and immediately after photosynthesis declined at ambient CO_2 as PEPC was inhibited (Fig. 3). The results show that the calculated BS resistances are similar to those obtained with the PEPC mutant. We measured A/C_i response curves (C_i determined from analysis of transpiration, which eliminates stomatal resistance) and calculated the resistance from the initial slope with V_c for Rubisco equal to 1.2 A_{max} estimated from CO_2-saturated rates in the presence of DCDP. In calculating r_{bs}, it is important to eliminate stomatal resistance and to account for any partial inhibition of Rubisco, and V_c, by DCDP. Jenkins et al. (1989a) calculated a permeability coefficient for CO_2 from the atmosphere to BS cells (the reciprocal for the total diffusive resistance, r_t) from measurements of photosynthetic O_2 evolution in the presence of DCDP at 1.6% (v/v) CO_2 by dividing the photosynthetic rate by the difference between atmospheric CO_2 (C_a) and estimates of C_{BS}. The calculated value of r_t from the study of Jenkins et al. in *A. edulis* is 556 s · cm^{-1} (or 1,373 m^2 s^{-1} mol^{-1}), which is about 10-fold higher than values of r_{bs} in the present study. Because r_t includes stomatal and BS-diffusive resistance, high stomatal resistance in excised leaves could contribute to high r_t values. Our A/C_i response curves with the PEPC mutant saturate sharply at intercellular CO_2 concentrations about 1%, whereas up to 5% (v/v) ambient CO_2 was required in experiments by Jenkins et al. (1989). Also, the calculation of r_t is dependent on input of V_c of Rubisco to calculate C_{BS}. Using the value of V_c from analysis of wild-type plants (Jenkins et al., 1989), rather than V_c in the presence of DCDP, will also overestimate V_c and the calculated diffusive resistance values (see also He and Edwards, 1996).

Light microscopy of leaf anatomy indicates that the wild-type plants grown under both 370 μbar and 10 mbar and the PEPC mutant grown under 10 mbar of CO_2 all have Kranz-type leaf anatomy (results not shown; Dever et al., 1995). In wild-type plants grown at 10 mbar of CO_2, the BS cell walls at the intercellular space are very thick relative to the walls of the

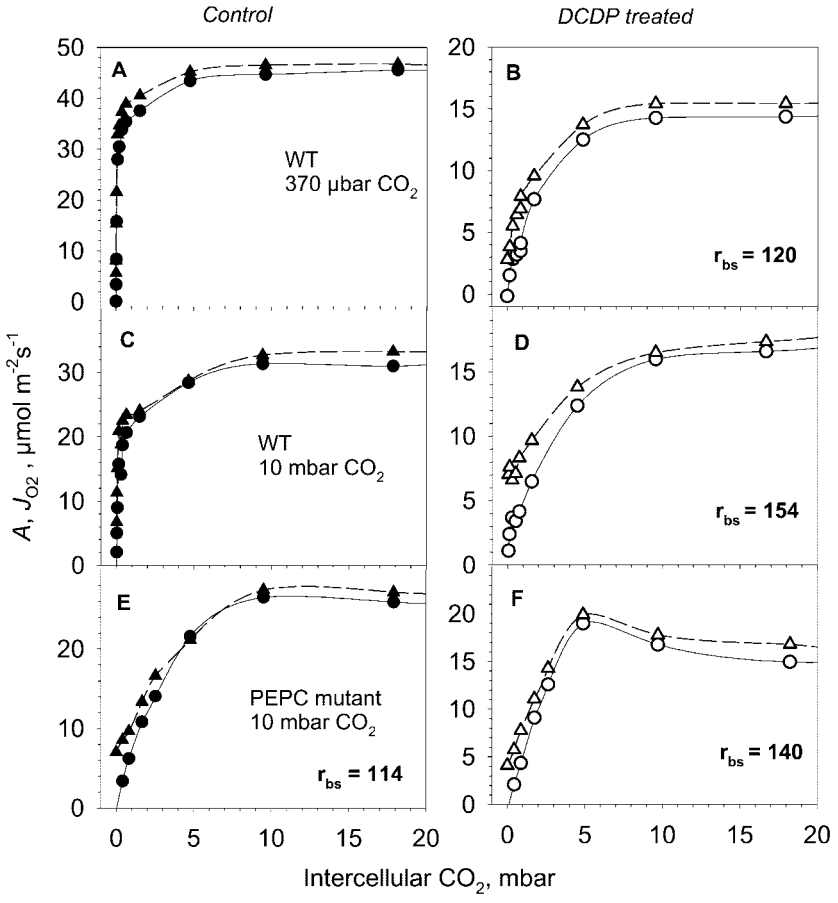

Figure 3. The response of the rates of CO_2 assimilation (*A*, ○, ●) and gross rate of O_2 evolution from PSII (J_{O2}, ▲, △) on wild type and PEPC mutant with and without feeding DCDP. Measurements were made on leaves of excised plants under 20 mbar O_2. The calculated values of r_{bs} in wild-type plants in presence of DCDP and in PEPC mutant with and without DCDP are shown. A and B, Wild-type plants grown at 370 μbar CO_2; C and D, wild-type plants grown at 10 mbar CO_2; E and F, PEPC mutant grown at 10 mbar CO_2.

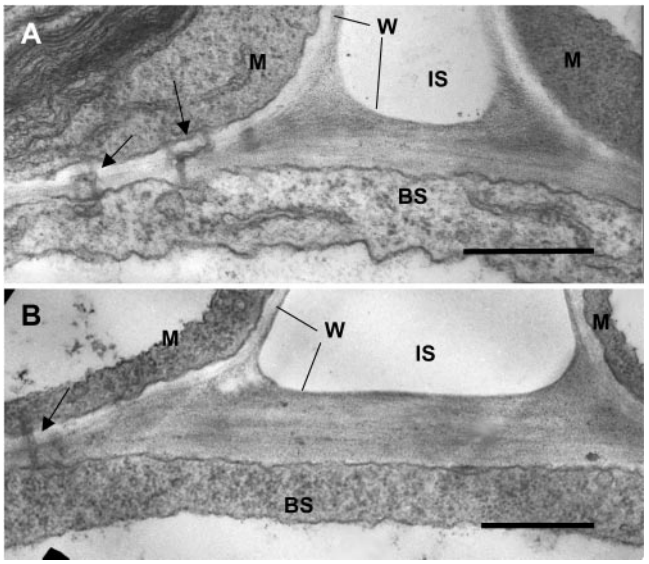

Figure 4. Electron microscopy showing cross sections through interface of mesophyll and BS of leaves of wild type (A) and PEPC mutant (B) with plants grown at 10 mbar CO_2. M, Part of mesophyll cell; BS, part of BS cell; W, cell wall; IS, intercellular air space. Arrows point to plasmodesmata. Scale bar = 0.5 μM. The average thickness of BS cell wall in contact with intercellular air from several sections was 0.34 μm for wild type and 0.32 μm for mutant (n = 3).

mesophyll and cross walls (Fig. 4); similar results were obtained with wild type grown under ambient CO_2. In the PEPC mutant, the BS cell walls are also much thicker than those of mesophyll cells, and cross walls include normal plasmodesmata (arrow). This suggests there are no structural differences between mutant and wild type.

Cellular Conductance and the Temperature Dependence of Photosynthesis under Limiting and Saturating CO_2

CO_2 response curves of photosynthesis were measured in wild-type and mutant *A. edulis* at leaf temperatures from 15°C to 35°C. Figure 5, A and B, describes the temperature response of A_{max}, determined from CO_2-saturated rates, and cellular conductance for CO_2, g, determined from the initial slope of the net rate of CO_2 assimilation (A/C_i) curves. In this case, conductance instead of resistance ($g = 1/r$) was used, because it is linearly related to the diffusion flux. In wild-type plants, the cellular conductance for CO_2, g_{wt}, was a function of liquid phase diffusion and carboxylation by PEPC in the mesophyll cell. For the mutant, g_{mut} was the total conductance from mesophyll to BS cells, including liquid phase (g_{bs}) and Rubisco (g_c), as determined earlier.

A_{max} increased with increasing temperature, with a Q_{10} value (the factor by which a reaction increases with a 10°C increase in temperature) of 2 for the mutant and 1.9 for the wild type between 20°C and 30°C. The corresponding activation energies were E_a = 13.5 and 11.3 kcal mol^{-1} (Fig. 5C, calculated between 20°C and 30°C). These values of Q_{10} and activation energies are as expected if photosynthesis under saturating CO_2 and light is controlled by enzymatic processes. Also, the activation energy for A_{max} in the mutant (13.5 kcal mol^{-1}) was close to the in vitro Rubisco activation energy of 13 kcal mol^{-1} (calculated from Jordan and Ogren, 1984). If RuBP is

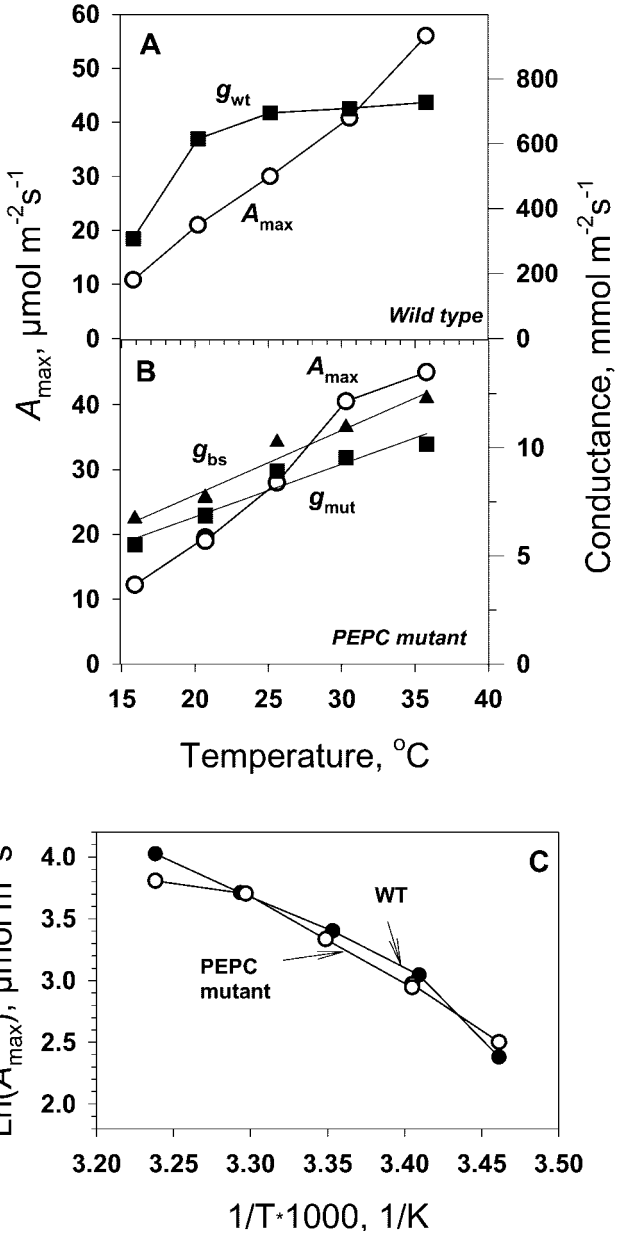

Figure 5. Temperature dependence of photosynthetic parameters for wild-type (A) and PEPC mutant (B) *A. edulis* measured under 0.3 mbar O_2. Shown are internal conductance in the mesophyll for wild type, g_{wt} (the initial slope of A/C_i curves), the internal conductance in the mutant, g_{mut}, and the calculated liquid phase-diffusive conductance in the mutant (g_{bs}) and maximal CO_2 assimilation rate (A_{max}). C has A_{max} from A and B plotted in Arrhenius axes (the slope equals $-E_a/R$). Values of $J_{O2\text{-net}}$ measured under saturating CO_2 (data not shown) were similar to values of A_{max}.

saturating for photosynthesis under high light, the Q_{10} values obtained would be consistent with Rubisco, rather than a diffusion limitation, being the major limiting factor for light- and CO_2-saturated photosynthesis in the mutant.

In the mutant, g_{mut} (which includes g_{bs} and Rubisco conductance) and g_{bs} had a linear response to increasing temperature. For g_{bs}, the Q_{10} values were 1.3 between 20°C and 30°C (Fig. 5B), which coincides with the temperature sensitivity of diffusion of small molecules in solutions that have a Q_{10} value of 1.3 (Nobel, 1991). The agreement between the measured and expected Q_{10} value for g_{bs} provides confidence that we are correctly measuring diffusive resistance of CO_2 to BS cells. Because CO_2 must diffuse to BS cells for fixation in the mutant, the cellular conductance values for the mutant are much lower than for the wild type.

In wild-type plants, CO_2 is fixed initially in mesophyll cells, and the temperature response of the mesophyll conductance, determined from the initial slope of the CO_2 response curve, showed a saturating curve rather than a linear response, indicating that biochemistry is involved (Fig. 5A). The effect of temperature on the initial slope of the A/C_i response in wild-type *A. edulis* depends on liquid phase diffusion and PEPC in mesophyll cells. The relative insensitivity of the mesophyll conductance in the wild type to temperature indicates control by biochemistry. This could be attributable to regulation of PEPC by temperature-dependent changes in K_m for phospho*enol*pyruvate (PEP; the substrate PEP is lower under limiting CO_2 [Leegood and von Caemmerer, 1988]), by allosteric effectors, and/or by covalent modification of the enzyme (phosphorylation/dephosphorylation). There also may be a temperature-dependent effect on PEP because the level is reported to increase with increasing temperature under normal atmospheric levels of CO_2 (Labate et al., 1990).

CO_2 Response and Partitioning of Photochemical Electron Flow

The CO_2 response curves for CO_2 fixation (A), gross rates of O_2 evolution (J_{O2}), and net rates of O_2 evolution ($J_{O2\text{-net}}$) of the mutant and wild-type leaves were measured at saturating light (Fig. 6). Measurements of A and J_{O2} were made at 210 mbar of O_2, representing current atmospheric levels, and measurements of A, J_{O2}, and $J_{O2\text{-net}}$ at near zero levels of O_2 (0.3 mbar), with an interest in studying O_2-dependent processes. To overcome the high-diffusive resistance from the atmosphere to the BS cells in the mutant, CO_2 concentrations as high as 2% (20 mbar) were required (Fig. 6, A and C), whereas near atmospheric levels were saturating for the wild type (Fig. 6, B and D). The mutant plants of *A. edulis* had about 100 times lower initial slopes in A/C_i curves compared with the wild type (Fig. 6, A versus B and C versus D). From various measurements of A_{max} at 30°C during the course of the study on young to mature leaves, values were usually 30 to 40 μmol m^{-2} s^{-1} in the mutant compared with 40 to 50 μmol m^{-2} s^{-1} in the wild type. It is apparent that rates of A, J_{O2}, and $J_{O2\text{-net}}$ were very similar in both the mutant and wild type at 0.3 mbar O_2 (Fig. 6, A and B). At 210 mbar of O_2, J_{O2} was substantially higher than A in both mutant and wild type (Fig. 6, C and D). This is clearly shown in Figure 6, E and F, where J_{O2}-A is plotted in response to varying CO_2 at 0.3 and 210 mbar of O_2. J_{O2}-A can potentially be accounted for by dark-type mitochondrial respiration (R_d), photorespiration (1.5 velocity of RuBP oxygenase [v_o]), photosystem (PS) II-dependent O_2 evolution associated with the Mehler-peroxidase reaction (J_{O2Mr}), and O_2 evolution associated with nitrogen assimilation (J_{O2NA}; see Eqs. 3–6).

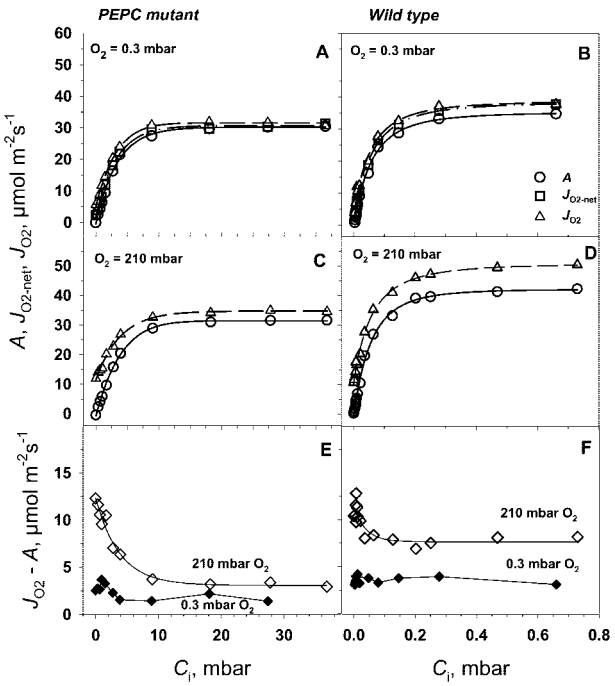

Figure 6. The response of the rates of CO_2 assimilation (A, ○), net O_2 evolution ($J_{O2\text{-net}}$, □), and gross O_2 evolution from PSII (J_{O2}, △) in PEPC mutant and wild-type *A. edulis* to intercellular CO_2 (C_i) at two oxygen partial pressures, 210 and 0.3 mbar. The CO_2 response curves were measured at PFD = 1,800 μmol m^{-2} s^{-1} and at leaf temperature 29°C.

In the mutant at 0.3 mbar of O_2, it is obvious that most of the PSII activity (J_{O2}) can be accounted for by CO_2 fixation and that R_d, v_o, J_{O2MR}, and J_{O2NA} must be low (Fig. 6, A and E). Because a partial pressure of 0.3 mbar of O_2 in the atmosphere is extremely low, a correspondingly low level is expected in the mesophyll cells within the leaf. However, even under very low external levels of O_2, the O_2 level in the BS cells will increase when O_2 is generated from PSII activity under a high-BS cell-diffusive resistance. At 0.3 mbar of O_2 in the atmosphere and based on the average

value for BS cell resistance determined in this study (described later), the calculated level of O_2 in BS cells at CO_2-saturated rates of photosynthesis was about 30 mbar. From Equation 14, if we take $A = 30$ μmol m^{-2} s^{-1}, $r_{bs} = 30$ s cm^{-1} (80 m^2 s^{-1} mol^{-1}), $a_w = 0.79$ (a_w is a constant that takes into account the difference in O_2 and CO_2 diffusivities [at 25°C, $a_w = 0.79$; Farquhar, 1983]), and $b = 0.5$, then the concentration of O_2 would be 35 μM (equivalent to about 30 mbar of O_2 in the gas phase; $O_2 = 0 + 0.79*0.5*30*A/10 = 35$ μM). R_d from measurements in the dark under normal atmospheric conditions is 2 to 3 μmol m^{-2} s^{-1} (data not shown). On average, J_{O2NA} for nitrate assimilation to Glu is estimated to be about 5% of A, not considering re-assimilation of ammonia from photorespiration (see Edwards and Baker, 1993). Thus, R_d in vascular tissue plus nitrate assimilation could easily account for the difference between J_{O2} and A at 0.3 mbar of O_2. Some rise in values of J_{O2}-A under limiting CO_2 at 0.3 mbar of O_2 would be expected, because A decreases relative to R_d (Fig. 6E). These results indicate that J_{O2Mr} and v_o must be very low in the mutant under 0.3 mbar of O_2 in the atmosphere.

In the mutant at 210 mbar of O_2, the values of J_{O2}-A were much greater than at 0.3 mbar of O_2, particularly with decreasing levels of CO_2 (Fig. 6E). The logical explanation for this effect is that the mutant, which lacks a C_4 cycle, has increasing rates of photorespiration under limiting CO_2 just as C_3 plants do (see also Lacuesta et al., 1997; Maroco et al., 1998a), which causes a corresponding increase in J_{O2}. Under high CO_2 and under 210 mbar of O_2, the mutant may have some additional dark-type respiration in mesophyll cells, resulting in larger values of J_{O2}-A than at 0.3 mbar of O_2.

In the wild-type plant under 0.3 mbar of O_2 (Fig. 6F), the value of J_{O2}-A was about 4 μmol m^{-2} s^{-1}, which was higher than in the mutant, and was independent of the level of CO_2. As with the mutant, nitrate assimilation and R_d in BS tissue may partly account for the difference. However, the Mehler reaction or photorespiration may also contribute in the wild-type plant. In a recent study, there was evidence for significant Mehler reaction in wild-type *A. edulis* under rather low levels of O_2 (between 0.2 and 20 mbar; Laisk and Edwards, 1998). In NAD-malic enzyme (NAD-ME) species like *A. edulis*, the Mehler reaction is proposed to function in mesophyll chloroplasts and contribute to generation of ATP for the C_4 cycle (Furbank and Badger, 1982; Laisk and Edwards, 1998). With increasing CO_2, there may be a rise in the rate of the Mehler reaction as the rate of the C_4 cycle increases, whereas with decreasing CO_2, there may be a rise in photorespiration; together these effects could result in values of J_{O2}-A being reasonably constant in NAD-ME-type species with varying CO_2 (see Furbank and Badger, 1982).

In the wild-type plant under 210 mbar of O_2, J_{O2} was higher than A across the CO_2 response curve (Fig. 6D); the pattern of change with increasing CO_2 is very similar to that of Canvin et al. (1980) from O_2 isotope analysis of photosynthesis in *A. edulis*. J_{O2}-A at 210 mbar was greater than at 0.3 mbar of O_2, and a sharp increase in J_{O2}-A occurred at very low levels of CO_2. Above approximately 0.025 mbar of CO_2, J_{O2}-A was constant at about 8 μmol m^{-2} s^{-1} (Fig. 6F). As noted above, this can be explained by O_2-dependent photorespiration at extremely low levels of CO_2 and increasing Mehler reaction at higher CO_2. The larger J_{O2}-A values at high CO_2 under 210 mbar versus 0.3 mbar of O_2 may be accounted for by O_2-dependent dark respiration and/or the Mehler reaction.

To evaluate Rubisco kinetics in mutant leaves relative to A and J_{O2}, we analyzed RuBP content and Rubisco activity (Fig. 7). With increasing CO_2 from zero up to about 0.8 mbar there was an increase in RuBP content, above which it decreased. The initial

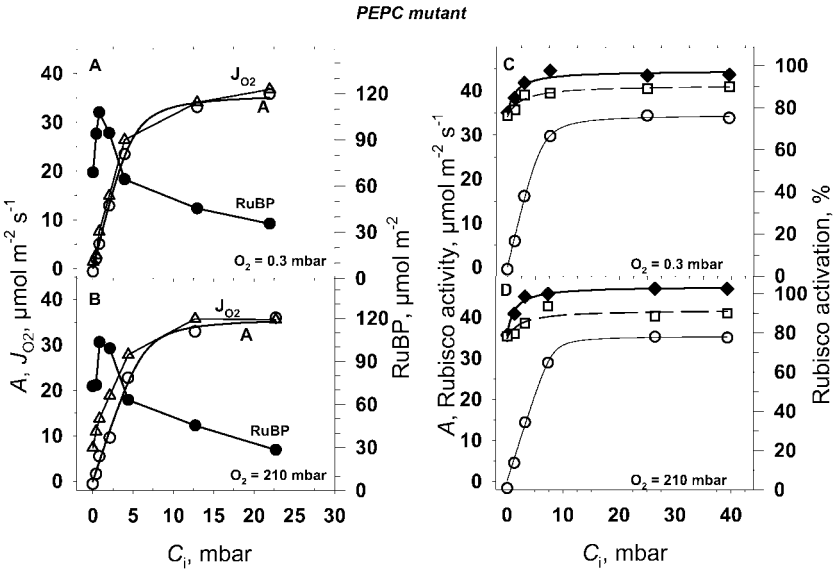

Figure 7. CO_2 response for CO_2 assimilation rate (A, ○), gross O_2 evolution rate (J_{O2}, △), RuBP pool size (●), Rubisco activity (◆), and Rubisco activation state (□) for PEPC mutant *A. edulis* at two O_2 pressures, 0.3 and 210 mbar. Leaf temperature was 28°C, PFD = 1,400 μmol m^{-2} s^{-1}. Each point is from a different leaf of similar age.

extractable activity of Rubisco in the mutant was higher than A_{max} at saturating CO_2 and decreased slightly at the lower CO_2 concentrations (Fig. 7, C and D). The decrease at low CO_2 correlated with a decrease in the state of activation of the enzyme. In the wild type (results not shown), leaf RuBP content was similar to the mutant at low CO_2 (at CO_2 = 34 μbar, RuBP was 56 μmol m^{-2}) and decreased at high CO_2 (at CO_2 = 4.8 mbar, RuBP was 47 μmol m^{-2}), which is in close agreement with the values of Leegood and von Caemmerer (1988). Considering a Rubisco active site turnover rate of 2.8 s^{-1} (Woodrow and Berry, 1988), the number of active sites per leaf area in *A. edulis* would be about 15 to 20 μmol m^{-2}. The RuBP concentration across the A/C_i curve at light saturation exceeded the number of active sites by about three times, which suggests the RuBP is at saturating levels. However, the observation that the RuBP concentration decreased at high CO_2 (Fig. 7) and with the known competitive interaction of some chloroplast metabolites with RuBP (e.g. PGA; Servaites and Geiger, 1995), it is possible that A_{max} is partly limited by RuBP regeneration.

Light Response and Partitioning of Photochemical Electron Flow

The response of photosynthesis to light under very high CO_2 (4%, 40 mbar) in the mutant gave about the same maximal quantum yield for O_2 evolution ($J_{O2\text{-net}}$, J_{O2}) as in the wild type (0.064 versus 0.066; Fig. 8, A and B). The quantum yield for O_2 evolution for wild-type *A. edulis* was higher than measured by Ehleringer and Bjorkman (1977) for CO_2 fixation in NAD-ME-type C_4 species (0.054). Higher values for the wild type may be explained by the use of highly saturating CO_2 and very low O_2, which would restrict O_2-dependent use of energy, and by the fact that O_2 evolution, rather than CO_2 uptake, was measured. In the wild-type plant under very high CO_2, the responses of J_{O2} and $J_{O2\text{-net}}$ to increasing light were very similar, indicating there was little photorespiration and Mehler reaction under this condition. It is uncertain why the Mehler reaction would be restricted under such high levels of CO_2 in the wild type. However, in the wild-type plant under 4% (v/v) CO_2, direct diffusion of CO_2 to BS cells would occur, bypassing the C_4 cycle, because in mutant plants, which lack a C_4 cycle, photosynthesis is saturated by 2% (v/v) CO_2.

In the mutant, under saturating levels of CO_2, which prevent photorespiration, we would expect maximum quantum yields of O_2 evolution similar to those of C_3 plants. Instead, the values in the mutant were lower than in C_3 plants under saturating CO_2 and similar to those of the *A. edulis* wild type. This suggests that the absorbed energy, which is used in the wild type in mesophyll chloroplasts for the C_4 cycle (ATP for conversion of pyruvate to PEP, and NADPH to the degree malate is synthesized), may be dissipated as heat in the mutant if there is no other means for using it in carbon assimilation. In the mutant, there is no requirement for energy in mesophyll cells in carbon assimilation, unless part of the PGA and glycerate formed via RuBP carboxylase and oxygenase activities in BS chloroplasts is shuttled to mesophyll cells for reduction (Fig. 1).

In the mutant under CO_2 which is limiting for photosynthesis (2 mbar), and at 210 mbar of O_2, J_{O2} was much higher than A, and the maximum quantum yield under limiting light was higher for J_{O2} than for A (Fig. 8C). This can be explained by the mutant having a high level of photorespiration and responding like a C_3-type species under limiting CO_2.

In the wild type under atmospheric levels of CO_2 and 210 mbar O_2, the light response curves showed a higher quantum yield (from initial slopes) and a higher light-saturated rate for J_{O2} than for A (Fig. 8D). This may be attributed to the Mehler reaction increasing with increasing light and generating ATP for the C_4 cycle under 210 mbar O_2, which could largely account for the difference between J_{O2} and A. With the wild-type plant having a functional C_4 cycle, photorespiration and dark-type respiration are expected to be minor components of the difference between J_{O2} and A. A previous study indicated that the Mehler reaction is functioning in *A. edulis* but is insufficient to supply the ATP needed to support the C_4 cycle (Laisk and Edwards, 1998). Thus, both the Mehler reaction and PSI-mediated cyclic electron flow may generate the ATP, with some flexibility in the magnitude of each. In contrast to results under

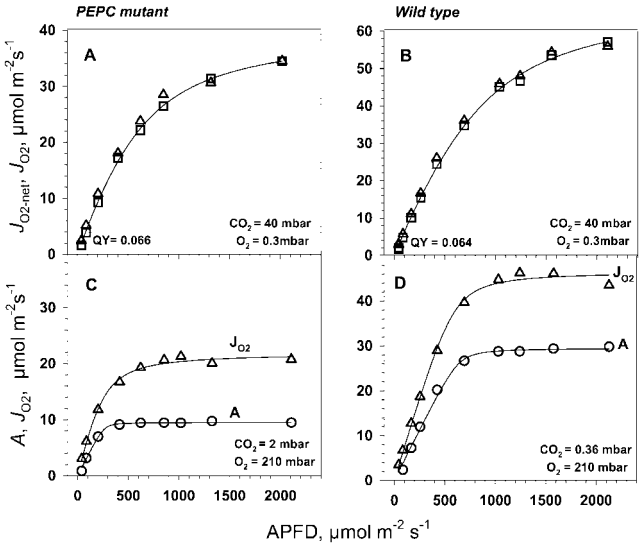

Figure 8. Light response of PEPC mutant and wild-type *A. edulis* O_2 evolution ($J_{O2\text{-net}}$, □) at highly saturating levels of CO_2 of 40 mbar CO_2 (O_2 = 0.3 mbar), and CO_2 uptake (A, ○) at limiting CO_2 (2 mbar for PEPC mutant and 0.36 mbar for wild type) and 210 mbar O_2 pressure. Leaf temperature was 28°C. Gross rates of O_2 evolution (J_{O2}, Δ) were calculated from simultaneous fluorescence measurements as described in "Materials and Methods."

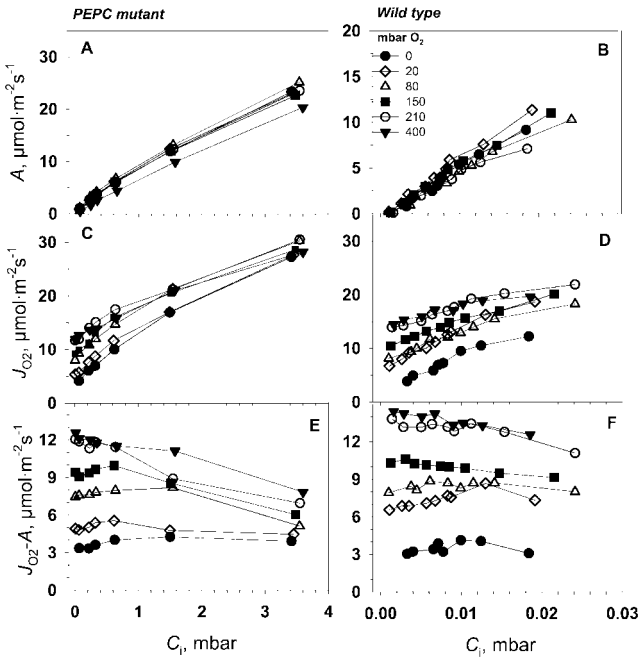

Figure 9. Oxygen sensitivity of *A. edulis* photosynthesis at limiting CO_2 concentrations, 30°C, and PFD = 1,800 μmol m^{-2} s^{-1}. The rate of PSII O_2 evolution (J_{O2}) shows an increase with increasing O_2 concentration and continues at CO_2 = 0 because of re-assimilation of CO_2 released from the photorespiration and from the Krebs cycle.

210 mbar of O_2 (Figs. 6D and 8D), there was no evidence for function of the Mehler reaction under low O_2 (Fig. 8B), which suggests the ATP needed to support the C_4 cycle is provided by PSI-dependent cyclic electron flow.

O_2 Effect on the Partitioning of Photochemical Electron Flow

It is well known that at low-CO_2 concentrations, the rate of CO_2 assimilation in C_4 plants exhibits low sensitivity to O_2. This is in contrast to C_3 plants, where photorespiration greatly reduces the rate of CO_2 assimilation in response to increasing O_2 (Kanai and Edwards, 1999). Measurements of A and J_{O2} in mutant plants, in which the C_4 cycle is not functional, provide an opportunity to follow more closely the maximum potential for Rubisco oxygenase and the glycolate pathway to function. This is not possible in normal C_4 leaves, where the CO_2 pump operates.

The responses of A and J_{O2} were measured at increasing O_2 concentrations over a range of CO_2-limited concentrations where greater RuBP oxygenase activity is expected for mutant and wild-type plants (Fig. 9). In the wild-type plant at rate-limiting CO_2 levels, high O_2 increased J_{O2}, but the CO_2 assimilation rates remained relatively unaffected by O_2 (Fig. 9, B and D). The increase in J_{O2} with increasing O_2 under low CO_2 suggests an increase in photorespiration through RuBP oxygenase activity. At a given level of O_2, the value of J_{O2}-A (Fig. 9F) remained about the same with increasing levels of CO_2, which, as discussed earlier, may be attributable to the Mehler reaction partially providing ATP to support the C_4 cycle and increasing with increasing rates of CO_2 fixation.

In the mutant, high O_2 increased J_{O2} at the lowest, rate-limiting CO_2 levels, but the CO_2 assimilation rates remained relatively unaffected by O_2 (Fig. 9, A and C). The increased electron transport rate with increasing O_2 under limiting CO_2 suggests an O_2-dependent increase in the RuBP oxygenation rate. At the higher levels of O_2, the difference between J_{O2} and A (Fig. 9E) was gradually suppressed by increasing CO_2, which is expected if increasing CO_2 suppresses photorespiration and considering that the mutant does not have a C_4 cycle that could be supported by the Mehler reaction.

For the mutant under limiting CO_2, the activity of J_{O2} is expected to be largely accounted for by the sum of the velocity of RuBP carboxylase (v_c) and v_o. We extrapolated J_{O2}, measured at different O_2 concentrations, to CO_2 = 0 and plotted the resulting values against BS cell O_2 concentration in an effort to evaluate the effect of Rubisco oxygenase activity on J_{O2} (Fig. 10). Assuming photorespired CO_2 is re-assimilated with the probability determined by the ratio of Rubisco conductance to BS cell conductance, the expected J_{O2} response can be described by the solid line in Figure 10. The experimental points are in good agreement with predicted results based on Rubisco kinetics if re-assimilation is accounted for, except that at the highest O_2 level (480 μM, which is

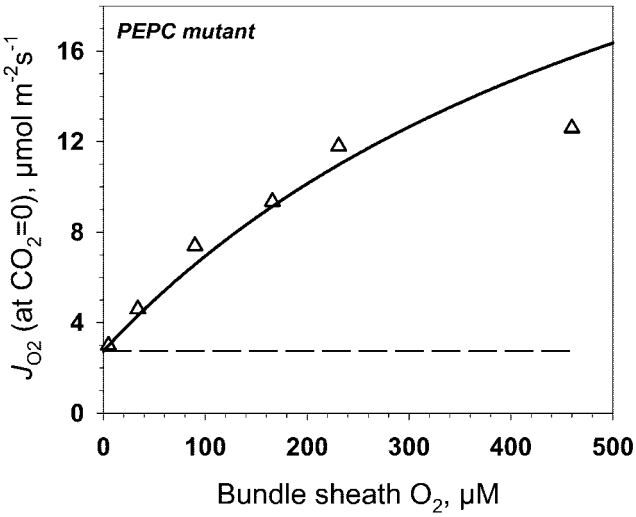

Figure 10. J_{O2} for the PEPC mutant of *A. edulis* from Figure 9 was extrapolated to CO_2 = 0, and the results were plotted against O_2 concentration. The simulated J_{O2} shown by the solid line was calculated based on BS O_2 and CO_2 concentration (the latter calculated for each O_2 level considering BS-diffusive resistance) and Rubisco kinetic constants (V_c = 39, K_c = 21 μM, and K_o = 640 μM), where J_{O2} equals v_c + v_o (Edwards and Baker, 1993). The rate of CO_2 re-assimilation (at zero external CO_2) is proportional to the ratio of Rubisco conductance and BS-diffusive conductance.

about twice the atmospheric level), the oxygenase activity was lower than expected. Analysis of RuBP content in the leaves of the mutant at low CO_2 (0.4 mbar) showed a decrease of RuBP concentration at rate-limiting CO_2 and with increasing O_2 (Fig. 11). Therefore, we suggest that the lower than expected J_{O2} value at O_2 concentration below the K_m for RuBP oxygenase (K_o) value (640 μM) in the mutant (Fig. 10) is the result of RuBP becoming partially limiting for CO_2 assimilation. Very similar results were obtained with wild-type plants (Fig. 11). Also, the response of J_{O2} to O_2, under low CO_2, in the wild type is similar to that in *A. edulis* measured at the CO_2 compensation point by O_2 isotope analysis (Canvin et al., 1980).

There was only a small effect of O_2 on the rate of CO_2 assimilation at low-CO_2 concentrations in either the mutant or wild-type *A. edulis* (Fig. 9). The limited effect of O_2 on CO_2 assimilation in the mutant, where there is no C_4 cycle function, can be explained by effective re-assimilation in the BS cells of the CO_2 that is generated from dark-type respiration and photorespiration. It is also evident that in the wild-type plants, CO_2 re-assimilation at low CO_2 affects assimilation kinetics. In this case, refixation of photorespired CO_2 may occur in mesophyll cells via PEPC, if there is leakage of CO_2, as well as in BS cells. However, the effectiveness of the mutant suggests that, under low CO_2, much of the photorespired CO_2 will be directly refixed in BS cells.

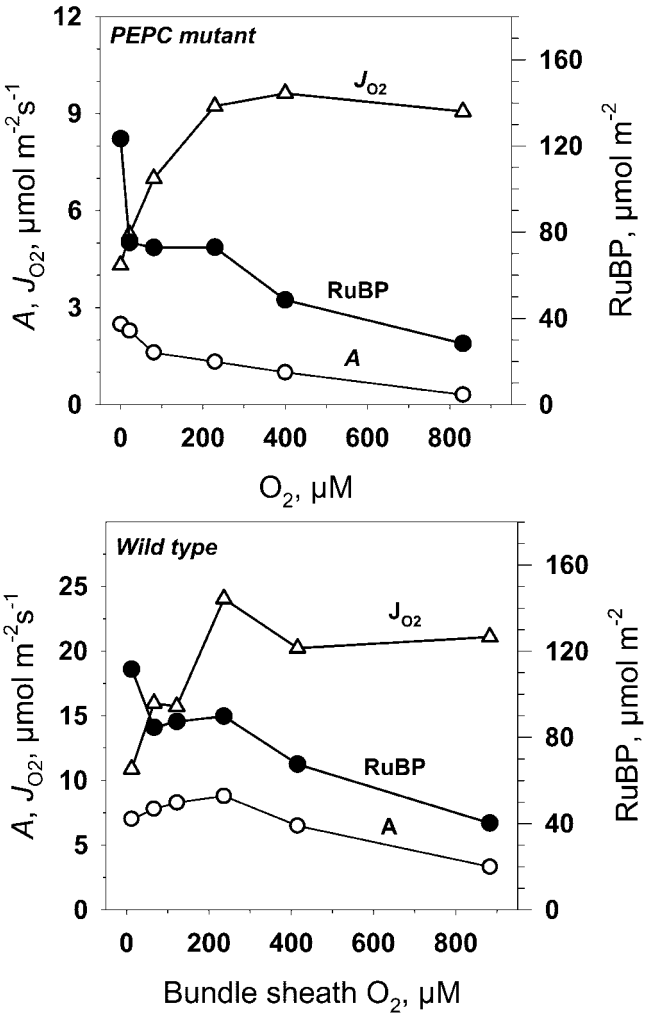

Figure 11. PEPC mutant and wild-type *A. edulis* leaf RuBP content (●) versus O_2 concentration with C_i of 0.4 mbar for mutant and 0.025 mbar for wild type. Also, CO_2 assimilation rate (*A*, ○) and O_2 evolution from PSII (J_{O2}, △) are shown. Leaf temperature was 28°C; light PFD = 1,800 μmol m^{-2} s^{-1}.

Calculation of CO_2 Concentration and Leakiness of CO_2 in BS Cells of *A. edulis*

If Rubisco kinetic parameters (V_c, K_c [the K_m for RuBP carboxylase], K_o, and S [the relative specificity factor for carboxylase versus oxygenase]) are known, one can calculate BS CO_2 concentration using a C_4 photosynthesis model (von Caemmerer, 2000). Figure 12 shows calculated BS cell CO_2 concentrations during photosynthesis in wild-type *A. edulis* leaves under varying intercellular CO_2 concentrations at 210 mbar of O_2 calculated with the model of C_4 photosynthesis. Also, shown in Figure 12 are the calculated values of BS cell leakiness during CO_2 fixation in wild-type plants, which range from approximately 0.2 to 0.3 (from Eqs. 16 and 17, using an r_{bs} value of 113 m^2 s^{-1} mol^{-1}). As increasing ambient levels of CO_2 became saturating for photosynthesis, the calculated levels of CO_2 in the BS cells of mature leaves reached levels of approximately 2,000 μbar, which is about six times that normally occurring in the atmosphere.

CONCLUDING REMARKS

The PEPC mutant of *A. edulis* has high light- and CO_2-saturated rates of photosynthesis comparable with those of the wild type. The high CO_2 required for growth and the high-diffusive resistance of the PEPC mutant to CO_2 indicate that physical restraints to gases have been conserved in the C_4 anatomy of the mutant. The value of BS cell resistance to CO_2 increased with leaf age in *A. edulis* from 72 to 181 m^2 s^{-1} mol^{-1} (Table I). Similar resistance values for mature leaves were obtained with wild-type plants treated with the PEPC inhibitor DCDP. The results suggest there may be developmental changes in BS cells that increase the diffusive resistance to CO_2 by changes in the liquid phase of the cell or cell wall properties. The concentration of CO_2 in BS cells under high rates of photosynthesis is estimated to be about six times current ambient levels, sufficient to largely repress photorespiration. Re-assimilation of CO_2 from dark-type respiration and photorespiration in BS cells is an important component of both PSII activity and consumption of reductive power at very low-CO_2 concentrations in *A. edulis*.

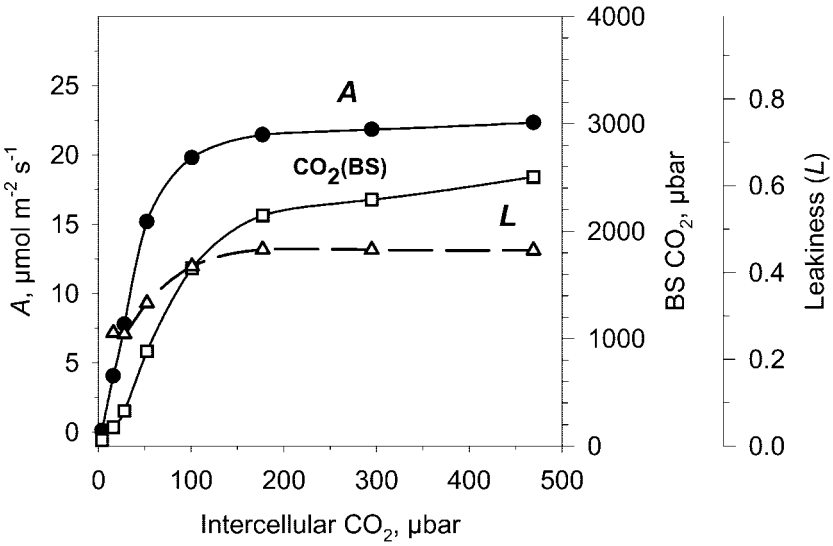

Figure 12. CO_2 response for CO_2 assimilation rate (at leaf temperature of 28°C; PFD = 1,800 μmol $m^{-2}s^{-1}$; ●), calculated CO_2 partial pressure in BS cells (□), and leakiness of CO_2 from BS cells (△). The CO_2 level in BS cells was calculated according to von Caemmerer (2000), and the leakiness was calculated according to equations 16 and 17 using r_{bs} value of 113 m^2 s^{-1} mol^{-1}. Similar results were obtained from analysis of several experiments on A/C_i responses.

MATERIALS AND METHODS

Growth Conditions

Mutant plants of *Amaranthus edulis* LaC_4 2.16 lacking PEPC activity and protein (Dever et al., 1995) were grown in growth chambers (Econair, Winnipeg, Canada) on fertilized potting soil in 8-L pots (one plant per pot), with a 14/10-h day/night cycle at 28°C/22°C, 50% relative humidity, 10 mbar of CO_2, and an incident photosynthetically quantum flux density (PFD) of 1,200 μmol m^{-2} s^{-1} light. Wild-type plants were grown under the same conditions, except the CO_2 concentration was 370 μbar and 10 mbar in experiments with DCDP and electron microscopy and 370 μbar in all other experiments.

Gas Exchange (A and $J_{O2\text{-}net}$)

Leaf gas exchange was measured with the FastEst gas system (FastEst, Tartu, Estonia; described in detail in Laisk and Oja, 1998). The system was equipped with a CO_2 analyzer (6251, LI-COR, Lincoln, NE) and a S-3A O_2 ceramic heated zirconium oxide analyzer (Applied Electrochemistry Inc., Sunnyvale, CA). Leaf gas exchange characteristics, net rates of CO_2 fixation (A), C_i, PFD, and leaf temperature were determined as in Laisk and Loreto (1996). For measurements of A under high levels of CO_2, there is an increase in noise to signal ratio in measuring CO_2 with an infrared gas analyzer. To improve measurements of A, sampling time was 0.1 s for 3 min resulting in 1,800 data points, which were averaged. For example, in one experiment A measured at 3% (v/v) CO_2 was 41.9 μmol m^{-2} s^{-1} with a SE with n = 1,800 of ± 0.12. The S-3A O_2 analyzer provides an accurate measure of the net rate of O_2 evolution ($J_{O2\text{-}net}$) under low levels of atmospheric O_2 (less than 10 mbar), independent of CO_2 concentration.

Measurement of Chlorophyll Fluorescence and Calculation of PSII Activity (J_{O2})

The yield of PSII was measured by chlorophyll fluorescence using a fluorometer (PAM 101, Walz, Effeltrich, Germany). The gross rate of O_2 evolution from PSII (J_{O2}) was calculated as:

$$J_{O_2} = \text{APFD}\cdot Y_{II}\cdot(F_m'-F_s)/F_m'/4 \quad (1)$$

where $(F_m'-F_s)/F_m'$ is the yield of PSII (e^- quanta absorbed), F_s is fluorescence yield of steady-state photosynthesis, F_m' is maximal fluorescence yield by exposure to a 1-s pulse of 15,000 μmol m^{-2} s^{-1} light and APFD is the absorbed photosynthetic quantum flux density at steady state (Genty et al., 1989). For estimating the relative optical cross section of PS II (Y_{II}), the method proposed by Laisk and Loreto (1996) was used. Y_{II} was found by extrapolating a plot of F_s/F_m' versus quantum yield of O_2 evolution measured with an O_2 electrode ($J_{O2\text{-}net}$) at different light intensities, to F_s/F_m' = 0. The measurements were made under a low-O_2 background (0.025%) and high CO_2 so that respiratory uptake of O_2 would be minimized and the O_2 evolution measured would reflect essentially all PSII activity. The calculated values of Y_{II} for wild-type and mutant plants were 0.44 to 0.55 and 0.41 to 0.48, respectively. For calculations of APFD, the light reflected and transmitted by the leaf was measured using an integrating sphere (Labsphere, North Sutton, NH). For the mutant leaf, the average fractional absorption of incident light was 0.82, whereas for the wild type, the value was 0.85. In mature leaves of mutant plants, the chlorophyll (a+b) content was 156 mg m^{-2} compared with 309 mg m^{-2} in the ambient CO_2-grown wild type. The fresh weights of the mutant and wild-type leaves were identical, 22 mg cm^{-2}, but the mutant had less dry weight per leaf area, 2.9 mg cm^{-2}, compared with 4.4 mg cm^{-2} in the wild type (leaves were sampled at midday).

Equations and Calculation of Leaf Photosynthesis Parameters

O_2 Evolution in Mutant and Wild Type

O_2 evolution associated with linear electron transport rate can be expressed as

$$J_{O_2} = v_c + v_o + J_1 \quad (2)$$

where v_c and v_o are RuBP carboxylation and oxygenation rates, respectively, and J_1 is the use of electrons in other processes (e.g. Mehler reaction and nitrogen reduction). The following equations illustrate the main factors in considering the relationship between J_{O2}, $J_{O2\text{-}net}$, and A in C_3 and C_4 plants, because there is no net consumption of reductive power in the C_4 cycle of malic enzyme-type species (see Edwards and Baker, 1993).

$$A = v_c - 0.5v_o - R_d \quad (3)$$

$$J_{O_2} = v_c + v_o + J_{O2Mr} + J_{O_2NA} \quad (4)$$

$$J_{O_2} = A + R_d + 1.5v_O + J_{O2Mr} + J_{O_2NA} \quad (5)$$

$$J_{O_2\text{-}net} = A + J_{O_2NA} \quad (6)$$

where R_d = rate of dark-type mitochondrial respiration, J_{O2Mr} = PSII-dependent O_2 evolution associated with the Mehler-peroxidase reaction, and J_{O2NA} = O_2 evolution associated with nitrogen assimilation (reduction of nitrate and assimilation to Glu).

Analysis of Parameters of CO_2 Fixation and r_{bs} in PEPC Mutant

We assume that light-saturated CO_2 uptake in the mutant *A. edulis* plants is limited primarily by physical diffusive resistance to CO_2 and Rubisco activity (see Fig. 1). Values for the diffusive resistance to CO_2, carboxylation resistance, and RuBP carboxylation and oxygenation velocities can be calculated from leaf gas exchange measurements using the biochemical model of Rubisco developed by Farquhar et al. (1980). According to their model for C_3 photosynthesis, the CO_2 assimilation rate in the mutant can be described according to equation 3 above, where $A = v_c - 0.5\ v_o - R_d$. Assuming Rubisco saturation by RuBP,

$$v_c = \frac{V_c \cdot C_c}{C_c + K_c(1 + O_c/K_o)} \quad (7)$$

$$v_o = \frac{V_o \cdot O_c}{O_c + K_o(1 + C_c/K_c)} \quad (8)$$

$$V_o = \frac{V_c \cdot K_o}{K_c \cdot S} \quad (9)$$

where V_c and V_o = maximum carboxylation and oxygenation velocities, respectively, K_c and K_o = carboxylation and oxygenation Michaelis constants, respectively, C_c and O_c = CO_2 and O_2 concentrations at Rubisco active sites, respectively, and S = Rubisco specificity for CO_2 relative to O_2. Total resistance to CO_2 flux in the mutant, r_t, can be described as the sum of three resistances

$$r_t = r_g + r_{bs} + r_c \quad (10)$$

where r_g is gas phase resistance (boundary layer and stomatal), r_{bs} is liquid phase resistance (effectively BS resistance), and r_c describes carboxylation resistance of Rubisco. Gas phase resistance, r_g, was calculated from transpiration data. Intercellular CO_2 partial pressure, C_i equals

$$C_i = C_a - r_g A \quad (11)$$

where C_a is ambient CO_2 and A is net CO_2 assimilation rate. Intercellular CO_2 partitions between the gas phase and the cell wall liquid phase, C_w is

$$C_w = \beta_c C_i \quad (12)$$

giving soluble CO_2 where β_c is the CO_2 solubilization coefficient. The CO_2 concentration at the sites of carboxylation in the mutant, C_c is

$$C_c = C_w - r_{bs} A \quad (13)$$

O_2 concentration in the BS chloroplasts can be described as

$$O_c = O_m + a_w \cdot b \cdot r_{bs} \cdot A \quad (14)$$

where O_2 concentration at the mesophyll cell wall is

$$O_m = \beta_o O_i \quad (15)$$

a_w is a constant that takes into account the difference in O_2 and CO_2 diffusivities (at 25°C $a_w = 0.79$; Farquhar, 1983), b is the relative proportion of O_2 evolution in BS cells, O_i is the intercellular concentration of O_2, and β_o is the O_2 partitioning factor between gaseous and liquid phase.

DCDP Feeding Experiments

A leaf petiole was cut under water, and the CO_2 response curve was measured at 2% (v/v) oxygen (Fig. 3, A–C). Water was then replaced by a 4 mM solution of DCDP (PEPC inhibitor). After DCDP caused a decrease of photosynthesis to a stable level under atmospheric levels of CO_2 (about 20 min), the CO_2 response was measured (Fig. 3, B, D, and F). Measurement of photosynthesis on excised leaves can be problematic; however, using the FastEst gas exchange system the A/C_i response curves could be run in 20 min. The maximum rates of CO_2 fixation and response curves of control plants were similar to intact plants.

Calculating BS Cell CO_2 Concentration and Leakiness in Wild-Type Plants

The mechanistic model of C_4 photosynthesis developed by von Caemmerer (2000) was used for estimating concentrations of CO_2 in BS cells. The model requires inputs for Rubisco kinetic parameters. The kinetic constants for *A. edulis* Rubisco (K_c = 16 μM, K_o = 640 μM, and S = 82 at 25°C) were obtained from the work of Jordan and Ogren (1983) and corrected for temperature according to Woodrow and Berry (1988). V_c was taken equal to the CO_2-saturated assimilation rate at a PFD of 1,800 μmol m^{-2} s^{-1}.

Leakiness of CO_2 from BS cells during photosynthesis in wild-type plants was calculated as a fraction of the rate of the C_4 cycle based on the above estimates of BS cell CO_2 concentration and measured values of r_{bs} in the *A. edulis* mutant, where the rate of leakage of CO_2 per unit leaf area (L_a) equals

$$L_a = ([CO_2]_{BS} - [CO_2]_i)/r_{bs} \quad (16)$$

with $[CO_2]_{BS}$ and $[CO_2]_i$ representing the level of CO_2 in BS cells versus the external concentration in the intercellular air space, respectively. Leakiness (L), from BS cells as a fraction of the rate of the C_4 cycle is defined as

$$L = L_a/(L_a + A) \quad (17)$$

Measurement of RuBP Content

Leaf metabolism was stopped by quick filling of the leaf chamber with cooled ethanol (approximately −90°C). The frozen leaf (8 cm^2) was then removed from the chamber and ground into a fine powder in a small mortar under liquid nitrogen. The powder was then transferred into 3 mL of 1 M $HClO_4$ and extracted for 15 min. The extract was neutralized with 5 M KOH and centrifuged 3 min at 5,000*g*. The supernatant was stored under liquid N_2 until analyzed. RuBP content was determined using the method of ^{14}C incorporation into acid stable product as in Prinsley et al. (1986) using purified Rubisco from tobacco (*Nicotiana tabacum*).

Rubisco and Chlorophyll Content

For Rubisco activity measurements, the leaves were sampled the same way as for RuBP determination. The frozen leaf powder was then transferred into CO_2-free 100 mM HEPES/KOH buffer (pH = 7.9). The Rubisco extraction buffer (1 mL per cm^2 of leaf) contained 20 mM $MgCl_2$, 2 mM EDTA, and 5 mM dithiothreitol. It was then ground and homogenized in a Broeck Tissue Grinder (Corning, Palo Alto, CA) for about 20 s and divided into two parts, the first of which was immediately assayed by injecting 0.1 mL into a 0.9-mL assay medium and running the reaction 30 s at 28°C. This was taken as the in vivo activity of Rubisco. The assay media had the following final composition: 100 mM HEPES/KOH (pH = 7.9), 10 mM Mg^{2+}, 2 mM EDTA, 5 mM dithiothreitol, 1 mM RuBP, and 10 mM $NaHCO_3$ + $NaH^{14}CO_3$ with specific activity of 0.5 C_i mol^{-1}. The second assay, which was run after incubating the enzyme preparation 15 min in the presence of 10 mM $NaHCO_3$, was taken as the fully carbamylated activity. It was shown, by adding purified Rubisco with known activities to leaf material before grinding, that there was no loss of activity attributable to extraction procedures. However, the possibility that some loss of activity may have occurred because of incomplete solubilization of Rubisco from the leaf material cannot be ruled out. The chlorophyll content of the leaves was determined according to Porra et al. (1989) using 80% (v/v) acetone extract.

ACKNOWLEDGMENTS

We thank Dr. Colin Jenkins (Commonwealth Scientific and Industrial Research Organization, Canberra, Australia) for providing PEPC inhibitor DCDP. We appreciate discussion and some preliminary work with Dr. João Maroco (Instituto Superior de Agronomia, Lisbon, Portugal) on this project.

Received May 8, 2002; returned for revision June 16, 2002; accepted June 30, 2002.

LITERATURE CITED

Brown RH (1997) Analysis of bundle sheath conductance and C_4 photosynthesis using a PEP-carboxylase inhibitor. Aust J Plant Physiol **24:** 549–554

Brown RH, Byrd GT (1993) Estimation of bundle sheath cell conductance in C_4 species and O_2 insensitivity of photosynthesis. Plant Physiol **103:** 1183–1188

Canvin DT, Berry JA, Badger MR, Fock H, Osmond CB (1980) Oxygen exchange in leaves in the light. Plant Physiol **66:** 302–307 concentrating mechanism and photorespiration. Plant Physiol **103:** 83–90

Dever LV, Blackwell RD, Fullwood NJ, Lacuesta M, Leegood RC, Onek LA, Pearson M, Lea PJ (1995) The isolation and characterization of mutants of the C_4 photosynthetic pathway. J Exp Bot **46:** 1363–1376

Edwards GE, Baker NR (1993) Can CO_2 assimilation in maize leaves be predicted accurately from chlorophyll fluorescence analysis? Photosynth Res **37:** 89–102

Edwards GE, Kiirats O, Laisk A, Okita TW (2000) Requirements for the CO_2 concentrating mechanism in C_4 plants relative to limitations on carbon assimilation in rice. *In* JE Sheehy, PL Mitchell, B Hardy, eds, Redesigning Photosynthesis in Rice. International Rice Research Institute, Philippines, and Elsevier Science BV, Amsterdam, pp 99–112

Ehleringer J, Bjorkman O (1977) Quantum yields for CO_2 uptake in C_3 and C_4 plants. Plant Physiol **59:** 86–90

Evans JR, von Caemmerer S (1996) CO_2 diffusion inside leaves. Plant Physiol **110:** 339–346

Evans JR, von Caemmerer S, Setchell BA, Hudson GS (1994) The relationship between CO_2 transfer conductance and leaf anatomy in transgenic tobacco with a reduced content of Rubisco. Aust J Plant Physiol **21:** 475–495

Farquhar GD (1983) On the nature of carbon isotope discrimination in C_4 species. Aust J Plant Physiol **10:** 205–226

Farquhar GD, von Caemmerer S, Berry JA (1980) A biochemical model of photosynthetic CO_2 assimilation in leaves of C_3 species. Planta **149:** 78–90

Furbank RT, Badger MR (1982) Photosynthetic oxygen exchange in attached leaves of C_4 monocotyledons. Aust J Plant Physiol **9:** 553–558

Furbank RT, Jenkins CLD, Hatch MD (1989) CO_2 concentrating mechanism of C_4 photosynthesis: permeability of isolated bundle sheath cells to inorganic carbon. Plant Physiol **91:** 1364–1371

Genty B, Briantais J-M, Baker NR (1989) The relationship between the quantum yield of photosynthetic electron transport and quenching of chlorophyll fluorescence. Biochim Biophys Acta **990:** 87–92

Hatch MD, Agostino A, Jenkins CLD (1995) Measurement of the leakage of CO_2 from bundle-sheath cells of leaves during C_4 photosynthesis. Plant Physiol **108:** 173–181

He D, Edwards GE (1996) Estimation of diffusive resistance of bundle sheath cells to CO_2 from modeling of C_4 photosynthesis. Photosynth Res **49:** 195–208

Henderson SA, von Caemmerer S, Farquhar GD (1992) Short-term measurements of carbon isotope discrimination in several C_4 species. Aust J Plant Physiol **19:** 263–285

Jenkins C, Furbank RT, Hatch M (1989a) Inorganic carbon diffusion between C_4 mesophyll and bundle sheath cells: direct bundle sheath CO_2 assimilation in intact leaves in the presence of an inhibitor of the C_4 pathway. Plant Physiol **91:** 1356–1363

Jenkins C, Furbank RT, Hatch MD (1989b) Mechanism of C_4 photosynthesis: a model describing the inorganic carbon pool in bundle sheath cells. Plant Physiol **91:** 1372–1381

Jordan DB, Ogren WL (1983) Species variation in kinetic properties of ribulose 1,5-bisphosphate carboxylase/oxygenase. Arch Biochem Biophys **327:** 425–433

Jordan DB, Ogren WL (1984) The CO_2/O_2 specificity of ribulose 1,5-bisphosphate carboxylase/oxygenase. Planta **161:** 308–313

Kanai R, Edwards GE (1999) Biochemistry of C_4 photosynthesis. *In* RF Sage, RK Monson, eds, The Biology of C_4 Photosynthesis. Academic Press, New York, pp 49–87

Ku MB, Edwards GE (1975) Photosynthesis in mesophyll protoplasts and bundle sheath cells of various types of C_4 plants: IV. Enzymes of respiratory metabolism and energy utilizing enzymes of photosynthetic pathways. Z Pflanzenphysiol **77:** 16–32

Labate CA, Adcock MD, Leegood RC (1990) Effect of temperature on photosynthetic carbon assimilation and contents of photosynthetic intermediates in leaves of maize and barley. Planta **181:** 547–554

Lacuesta M, Dever V, Munoz-Rueda A, Lea PJ (1997) A study of photorespiratory ammonia production in the C_4 plant *Amaranthus edulis*, using mutants with altered photosynthetic capacities. Physiol Plant **99:** 447–455

Laisk A, Edwards GE (1998) Oxygen and electron flow in C_4 photosynthesis: Mehler reaction, photorespiration and CO_2 concentration in the bundle sheath. Planta **205:** 632–645

Laisk A, Edwards GE (2000) A mathematical model of C_4 photosynthesis: the mechanism of concentrating CO_2 in NADP-malic enzyme type species. Photosynth Res **66:** 199–224

Laisk A, Loreto F (1996) Determining photosynthetic parameters from leaf CO_2 exchange and chlorophyll fluorescence. Plant Physiol **110:** 903–912

Laisk A, Oja V (1998) Dynamics of Leaf Photosynthesis. Commonwealth Scientific and Industrial Research Organization Publishing, Collingwood, Australia

Leegood RC, von Caemmerer S (1988) The relationship between contents of photosynthetic metabolites and the rate of photosynthetic carbon assimilation in leaves of *Amaranthus edulis* L. Planta **174:** 253–262

Maroco JP, Ku MSB, Furbank RT, Lea PJ, Leegood RC, Edwards GE (1998a) CO_2 and O_2 dependence of PSII activity in C_4 plants having genetically produced deficiencies in the C_3 and C_4 cycle. Photosynth Res **58:** 91–101

Maroco JP, Ku MSB, Lea P, Leegood R, Furbank R, Edwards GE (1998b) Oxygen requirement and inhibition of C_4 photosynthesis: an analysis of C_4 plants deficient in the C_3 and C_4 cycles. Plant Physiol **116:** 823–832

Nobel PS (1991) Physicochemical and Environmental Plant Physiology. Academic Press, New York

Porra RJ, Thompson WA, Kriedemann PE (1989) Determination of accurate extinction coefficients and simultaneous equations for assaying chlorophyll *a* and *b* with four different solvents: verifications of the concentrations of chlorophyll standards by atomic absorption spectroscopy. Biochim Biophys Acta **975:** 384–394

Prinsley RT, Dietz K-J, Leegood RC (1986) Regulation of photosynthetic carbon assimilation in spinach leaves after a decrease of irradiance. Biochim Biophys Acta **849:** 254–263

Servaites JC, Geiger DR (1995) Regulation of ribulose 1,5-bisphosphate carboxylase/oxygenase by metabolites. J Exp Bot **46:** 1277–1283

von Caemmerer S (2000) Biochemical Models of Leaf Photosynthesis. Commonwealth Scientific and Industrial Research Organization Publishing, Collingwood, Australia

Woodrow IE, Berry JA (1988) Enzymatic regulation of photosynthetic CO_2 fixation in C_3 plants. Annu Rev Plant Physiol Plant Mol Biol **39:** 533–594